



**Environmental
Science**
Processes & Impacts

**The Fate of Inhaled Uranium-Containing Particles upon
Clearance to Gastrointestinal Tract**

| | |
|---------------|---|
| Journal: | <i>Environmental Science: Processes & Impacts</i> |
| Manuscript ID | EM-ART-05-2022-000209.R1 |
| Article Type: | Paper |
| | |

SCHOLARONE™
Manuscripts

The Fate of Inhaled Uranium-Containing Particles upon Clearance to Gastrointestinal Tract

Eshani Hettiarachchi¹, Milton Das¹, Daniel Cadol², Bonnie A. Frey³, and Gayan Rubasinghe^{1*}

1. Department of Chemistry, New Mexico Institute of Mining and Technology, 801 Leroy Place, Socorro, NM 87801

2. Department of Earth & Environmental Sciences, New Mexico Institute of Mining and Technology, 801 Leroy Place, Socorro, NM 87801

3. New Mexico Bureau of Geology and Mineral Resources, New Mexico Institute of Mining and Technology, 801 Leroy Place, Socorro, NM 87801

Abstract

Uranium-bearing respirable dust can cause various health problems, such as cardiovascular and neurological disorders, cancers, immunosuppression, and autoimmunity. Exposure to elevated levels of uranium is linked to many such health conditions in Navajo Nation residents in northwestern New Mexico. Most studies have focused on the fate of inhaled dust particles ($< 4 \mu\text{m}$) in the lungs. However, larger-sized inhaled particles ($10 - 20 \mu\text{m}$) can be cleared to the human gastrointestinal tract (GIT), thereby enabling them to interact with stomach and intestinal fluids. Despite the vital importance of understanding the fate of uranium-bearing solids entering the human GIT and their impact on body tissues, cells, and gut microbiota, our understanding remains limited. This study investigated uranium solubility from dust and sediment samples collected near two uranium mines in the Grants Mining District in New Mexico in two simulated gastrointestinal fluids representing fasting conditions in the GIT: Simulated Gastric Fluid (SGF) and Simulated Intestinal Fluid (SIF). The dissolution of uranium from dust depends on its mineralogy, fluid pH, and composition. The dust samples from the Jackpile mine favored higher solubility in the SIF solution, whereas the sediment samples from the St. Anthony mine favored higher solubility in the SGF solution. Further, geochemical calculations performed with the PHREEQC modeling program suggested that samples rich in the minerals andersonite, tyuyamunite, and/ or autunite have higher uranium dissolution in the SIF solution than in the SGF solution. We also tested the effect of added kaolinite and microcline, which are both present in some samples. The ratio of dissolved uranium in SGF relative to SIF decreases with the addition of kaolinite for all mineral phases but andersonite. With the addition of microcline, the ratio of dissolved uranium in SGF relative to SIF decreases for all the tested uranium minerals. The most prevalent oxidation state of dissolved uranium was computationally determined as +6, U(VI). The geochemical calculations made with PHREEQC agree with the experimentally observed results. Therefore, this study gives insight into the mineralogy-controlled toxicological assessment of uranium-containing inhaled dust cleared to the gastrointestinal tract.

Keywords: windblown dust, inhalation, gastric fluid, intestine fluids, genotoxicity, health risks

Environmental Significance Statement: In places where uranium mining occurred, the windblown dust contains a significantly higher quantity of uranium than the background levels. Many studies are focused on understanding the fate of this uranium in human lungs once inhaled. However, the relatively larger-sized inhaled particles clear into the human digestive system. Here, we focus on understanding the fate of uranium in inhaled dust in the simulated human stomach and intestine. We report that the uranium leaching in the stomach is primarily dependent on the mineralogy of dust inhaled. Therefore, we state that the toxicological studies of inhaled uranium should be site-specific. Furthermore, the dust mineralogy and body conditions should be considered when assessing their toxicology.

Introduction

Uranium (U) is the heaviest naturally occurring metal and is radioactive.¹ Being a heavy metal, its chemical toxicity is independent of the radioactivity-related toxicity and thus cannot be overlooked.² The established maximum U contamination level in drinking water is 30 ppb.³ Exposure to higher contamination levels can cause cardiovascular and neurological disorders, cancers, immunosuppression, and autoimmunity.^{3–6} During exposure to depleted uranium, uranyl cation (UO_2^{2+}) binds to DNA in mammalian cells, forming a uranium-DNA (U-DNA) adduct that could cause mutations, thereby triggering a range of protein synthesis errors, some of which may lead to various cancers.^{7–10} A study on rat epithelial cells showed that uranium might induce significant oxidative stress and a concomitant decrease in the anti-oxidative potential of lung tissues.^{8–11} Another study discusses the death of macrophages when exposed to UO_2^{2+} .¹² While these studies were conducted with aqueous phase uranium, others have reported that insoluble uranium oxide particles (e.g., UO_2) may cause the breakdown of DNA double strands in bronchoalveolar lavage cells.^{8,13,14} A recent study showed that exposure to mine-site derived particulate matter (PM) containing uranium-containing particles exacerbates neurological and pulmonary inflammatory outcomes in an autoimmune mouse model.¹⁵ One sample site used in the study, St. Anthony mine, New Mexico, was also used as a study site for our current study.

Several studies suggest that humans are primarily exposed to uranium through inhalation.^{16–18} Airborne particulate matter with a complex chemical composition becomes more inhalable as particle size decreases. While smaller particles ($< \sim 4 \mu\text{m}$) reach the deep lung environments, particulate matter of larger sizes ($10 \mu\text{m} - 100 \mu\text{m}$) can be cleared into the gastrointestinal tract (GIT).^{17,19–22} Furthermore, the number of particles cleared from the nose to the GIT can be as high as 50% of the deposit.^{20,22} The GIT is a critical organ with high absorbance capacity that is comprised of multiple tissues that are home to diverse and abundant essential immune cells and microbiota.^{3,18} Therefore, studies are required to investigate the exposure and toxicity of uranium in the GIT following clearance from the inhalation route.^{17,23} Although the absorption of solid uranium species in the GI tract is relatively poor, the efficiency increases with the increased solubility.^{2,24} On average, 1–5 μg of uranium are ingested daily through food and water consumption, whereas only 0.5 – 5% of the uranium ingested is usually absorbed.^{2,25} Human daily doses are two to three times higher in contaminated areas such as those near mine sites.² In the

1
2
3 current study, the leaching capacity of uranium from inhaled dust that may be cleared to the
4 gastrointestinal tract is investigated using two different simulated gastrointestinal fluids. The two
5 fluids are simulated gastric fluid (SGF) and simulated intestinal fluid (SIF). They simulate the
6 stomach environment and the human intestine conditions, respectively, in the fasted state.²⁶ The
7 compositions of these fluids are provided in the **Supporting Information, Table S1**.
8
9

10 Toxicity studies on inhaled uranium cleared to the digestive tract are relatively scarce. However,
11 uranium entering the digestive tract can damage the kidneys, causing toxicity.^{2,27} A recent study
12 reported that exposure to dissolved uranium through the GI tract causes significant immunotoxicity
13 among male and female mice.³ Another study concluded that the absorption of uranium by the
14 digestive tract does not significantly influence the chemical speciation of dissolved uranium.²⁵
15 Further, numerous previous studies have linked heavy metal exposure^{28–31}, including uranium³, to
16 disruptions of the gut microbiota that are crucial for maintaining systemic immune health. On the
17 other hand, Cleveland et al. suggested that the gut microbiota may take up uranium and act as a
18 barrier between the body and the uranium in the stomach, thereby reducing the overall impact of
19 uranium on tissue cells.³² The contrasting conclusions within the scientific literature call for further
20 studies on the topic.
21
22
23
24

25 In recent decades, a notable increase in cardiovascular and metabolic diseases in the Navajo
26 population residing close to the Grants Mining District (GMD), New Mexico, has been observed,
27 with only limited investigations into possible contributions from environmental contaminants, in
28 particular uranium and vanadium.³³ In a previous study, we investigated uranium exposure via
29 dust inhalation and subsequent dissolution in simulated human lung environments in relation to
30 the source of the dust.³⁴ In this study, we employed similar methods in understanding the fate of
31 solid uranium-bearing particles cleared to the human gastrointestinal tract. This study further
32 focuses on the mineralogy of uranium and major non-uranium minerals present in the dust
33 collected near mine sites in the GMD. In addition to laboratory simulations, a geochemical
34 modeling software program, PHREEQC 3.3.8, was used to further investigate the effect of
35 mineralogy on the dissolution of uranium in these simulated fluids.³⁵ By the combined results of
36 laboratory studies and computational-geochemical studies, we report that the mineralogy of
37 uranium-bearing dust impacts the extent of dissolution of uranium in these simulated body
38 conditions. Further, we report that a synergistic impact of multi-mineral composition plays a vital
39 role in uranium mobilization in the solutions, thus, attributing solubility and toxicity trends to a
40 single mineral phase can cause errors in toxicity assessments. However, it is important to mention
41 that the toxicity of undissolved particulate matter has not taken into account in this study.
42
43
44
45
46
47
48

49 **Materials and Methods**

50 *Dust and Sediment Sample Collection*

51 Dust and sediments were collected from four sites near Jackpile and St. Anthony mines, within ~5
52 km of communities in the GMD, New Mexico. Rock and sediment samples were collected from
53 an un-reclaimed open pit at St. Anthony mine (35.1562 N latitude, 107.2940 W longitude) during
54
55
56
57

1
2
3 the summer of 2017. Passive dust collectors (Big Spring Number Eight dust flux samplers),
4 installed 0.25 m above the ground surface, collected samples from November 2016 to August 2017
5 at three locations near the mines: site M, within a reclaimed pit at Jackpile mine (35.1240 N,
6 107.3705 W); site K, 3 km downwind of both reclaimed and un-reclaimed mine pits (35.1298 N,
7 107.2929 W); and site L, 4 km downwind (35.1259 N, 107.2859 W). (**Supporting Information,**
8 **Figure S1**) The collected samples from dust sites M, K, and L, and from the St. Anthony mine
9 were sieved with a 500 μm US standard sieve to remove any organic debris before use in
10 dissolution studies. Sieved samples of the size fraction less than 20 μm were used for dissolution
11 studies in Simulated Gastrointestinal Fluids (SGIF).
12
13
14
15

16 *Standards & Chemicals*

17
18 All chemicals were reagent grade or better and used as received. A standard sample of U_3O_8 from
19 the National Bureau of Standards (NIST, Assay 99.9%) was used as a proxy in this study. All the
20 solutions and the media were prepared in purified water (18.2 M Ω , Milli-Q-A10). The following
21 chemicals were used to prepare simulated gastrointestinal fluids according to the composition
22 described in Marques et al., 2011.²⁶ The chemicals are sodium taurocholate ($\text{C}_{26}\text{H}_{44}\text{NNaO}_7\text{S}$,
23 Beantown Chemicals, 97%), lecithin ($\text{C}_{42}\text{H}_{80}\text{NO}_8\text{P}$, VWR Chemicals, High purity grade), pepsin
24 (VWR Chemicals, Biotechnology grade), maleic acid ($\text{C}_4\text{H}_4\text{O}_4$, TCI, +99.0%), sodium chloride
25 (NaCl , Acros, +99%), sodium hydroxide (NaOH , VWR International, 97%), and hydrochloric acid
26 (HCl , VWR International, ACS grade/36.5-38.0%).
27
28
29
30

31 *Characterization of Dust Samples*

32
33 The surface areas of samples were measured in a seven-point N_2 -Brunauer-Emmet-Teller (BET)
34 isotherm using a Quantachrome Autosorb-1 surface area analyzer. Samples were outgassed
35 overnight (~24 h) at a temperature of 105°C prior to the BET analysis. The particle size of the
36 sieved samples was measured using SEM images. (**Supporting Information, Figures S2 and S3**)
37 To determine the elemental concentrations of each dust sample, an acid digestion procedure was
38 followed. A 0.2 \pm 0.01 g subsample was weighed from each sample and placed in an individual
39 digestion tube. Before analysis, samples were sieved through a 500 μm sieve to remove organic
40 debris. A 3 mL of trace-metal-grade hydrofluoric acid and 9 mL of trace-metal-grade nitric acid
41 were added to each digestion tube, and each tube was capped and placed in a holder. A preset
42 microwave routine (Milestone EthosUP) included a 25-minute ramp to 180°C, after which the
43 oven held that temperature for 10 minutes, consistent with the EPA 3052b digestion method.³⁶
44 Major, minor, and trace elements were quantified using inductively coupled plasma-mass
45 spectroscopy (ICP-MS, Agilent 7900).
46
47
48
49

50
51 X-ray diffraction (XRD) analyses of dust samples were performed in a Pananalytical X'Pert Pro
52 Diffractometer equipped with a copper source. Due to the total %U of these samples being lower
53 than 1% (the usual detection limit of the XRD analysis), a pre-concentration procedure was carried
54 out. Briefly, the dust samples were first sieved through a 500 μm US standard sieve to remove
55 debris. The uranium minerals in these samples are coatings around the quartz grains. Therefore,
56
57
58
59
60

1
2
3 the particles were lightly scratched using a porcelain pestle to scrape out the uranium minerals
4 while sieving. Additional sieving was carried out using 120 μm , 45 μm , and 20 μm US standard
5 sieves. The finest fraction collected was analyzed with XRD. Then, the spectra were compared
6 with 15 different common uranium minerals in New Mexico along with common major minerals
7 (i.e., quartz, kaolinite, microcline, dolomite, calcite, and rutile). The presence of uranium minerals
8 was confirmed only when their intensities and d – spacing were matched with respective standard
9 patterns with at least five major peaks. Additional information on this method is provided in our
10 previous study.³⁴
11
12
13

14 ***Dissolution of Uranium in Simulated Gastrointestinal Fluids***

15
16 Dissolution studies were carried out in a custom-built glass reactor inside a dark room to measure
17 the total dissolved uranium concentration (TDU). The capacity of the reaction vessel was 100 mL
18 with a removable airtight top. The sample loading was 20 mg in 100 mL of the simulated fluids.
19 During the reaction, the temperature was maintained at 37°C using a heated water jacket, and the
20 reaction mixture was in continuous agitation by using a magnetic stirrer. The sample aliquot of ~2
21 mL was collected periodically using a disposable syringe connected to a 12 cm Teflon tubing. The
22 collected samples were centrifuged and filtered via 0.2 μm syringe filters before analyzing them
23 with ICP-MS to avoid solid carryovers. All dissolution studies were performed in triplicate, and
24 mean TDUs have been reported with the standard deviation. The pH of the media was measured
25 before and after each dissolution experiment.
26
27
28
29

30 ***Detection of Uranyl Cation Formation***

31
32 A Uranyl-Curcumin-Triton-X System was prepared according to the method described by Zhu et
33 al.³⁷ The calibration standards were prepared using 400 μM stock uranyl acetate solution prepared
34 in SGF and SIF matrices. Extended information on this method is provided in our previous study.³⁴
35 However, the UV-VIS absorption of two stock solutions made on SGIFs (Simulated Gastro
36 Intestinal fluid) was compared with a MilliQ water-based stock solution using Evolution 200 UV
37 – Vis Spectrometer to confirm that there was no significant interference from the matrix.
38
39
40

41 ***Geochemical Modeling***

42
43 PHREEQC 3.3.8 with a modified MINTEQ database was employed in geochemical modeling.³⁵
44 In the database, taurocholate is represented by taurine and pepsin as glycine in order to incorporate
45 essential thermodynamic parameters. The maximum dissolved uranium concentration at
46 equilibrium in an oxidizing atmosphere in the two simulated gastrointestinal fluids was calculated
47 for identified uranium minerals and total site mineralogy. These model calculations were singular,
48 and no replicates were conducted. Further, changes in uranium solubility in the presence of
49 kaolinite or microcline for each uranium mineral were investigated. Kaolinite was detected as a
50 major mineral in all tested samples, whereas microcline was detected in all samples except the St.
51 Anthony sediment sample. For individual uranium minerals, excess of the mineral in 100mL of
52 the gastrointestinal fluids in oxidized conditions at 37°C was considered. For simulations with the
53
54
55
56
57
58
59
60

site mineralogy, molar ratios of minerals were selected based on the XRD peak intensities. The SGF and SIF input files are provided in **Supporting Information**.

Results and Discussion

Particle Characterization

The particles used in this study were sieved prior to use. The particle sizes were analyzed from SEM images with the software package ImageJ. The average particle sizes were 9.32 ± 4.54 , 15.97 ± 7.8 , 10.21 ± 5.10 , 12.72 ± 7.05 , and 3.64 ± 2.49 μm in diameter for the samples from Site K dust, Site L dust, Site M dust, St. Anthony sediment, and St. Anthony rock respectively. The SEM images with their respective particle-size distributions are reported in the Supporting Information (**Figures S2 and S3**). The sieving was conducted softly, and mild physical abrasion was employed. The measured surface areas and %U of each dust sample after sieving are provided in **Table 1**. All but the St. Anthony samples contain less than 0.40% total uranium. St. Anthony sediment and rock samples contain 0.87% and 4.42% U respectively. As revealed from XRD analysis (**Table 2**), the uranium mineralogy of these samples is a combination of commonly found uranium minerals in the area.^{34,38}

Dissolution of Uranium in Simulated Gastrointestinal Fluids

Inhalation of airborne dust particles poses a great health risk to humans, as these dust particles often contain toxic heavy metals.³⁹ While the finer fraction of these particles reaches the deeper lung and interacts with human lung fluids, the larger particles may clear to the human digestive system.¹⁷ Once cleared to the human digestive system, these dust particles are likely to interact with fluids in the stomach and intestine.^{18,40,41} Although, in human body conditions, materials in the stomach first interact with gastric fluids, and the undigested remainder passes to the human intestine, in our bench experiments, a fresh sample was used each time for the two different gastrointestinal fluids. This was to keep the experiments simple enough to understand the uranium leaching capacity and possible mechanisms. In the fasted state, the stomach contains about 40 mL of capacity.²⁶ The 20 mg of dust used in 100 mL in our experiments roughly converts to 8 mg of dust exposure within 24 hours.

Table 1: Surface area analysis and the %U analysis of the uranium-containing samples.

| Sample | Source of the samples | 7 points N ₂ BET surface area (m ² /g) | %U |
|-------------------------------|------------------------------|--|------|
| U ₃ O ₈ | National Bureau of Standards | 0.46±0.04 | 85 |
| St. Anthony sediment | St. Anthony Mine | 1.61±0.08 | 0.87 |
| St. Anthony rock | St. Anthony Mine | 134.15±1.58 | 4.42 |
| Site K dust | Jackpile Mine | 31.85±0.41 | 0.38 |
| Site L dust | Jackpile Mine | 38.85±1.10 | 0.12 |
| Site M dust | Jackpile Mine | 36.26±1.46 | 0.10 |

Table 2: Identified minerals in the samples with XRD analysis. √ Indicates they were identified.

| Sample | Chemical Formula | St. Anthony sediment | St. Anthony Rock | Site K | Site L | Site M |
|------------------------|--|----------------------|------------------|--------|--------|--------|
| Major Minerals | | | | | | |
| Quartz | SiO ₂ | √ | √ | √ | √ | √ |
| Dolomite | CaCO ₃ .MgCO ₃ | √ | -- | √ | √ | √ |
| Microcline | KAlSi ₃ O ₈ | -- | √ | √ | √ | √ |
| Kaolinite | Al ₂ Si ₂ O ₅ (OH) ₄ | √ | √ | √ | √ | √ |
| Rutile | TiO ₂ | √ | -- | -- | -- | -- |
| Trace Uranium Minerals | | | | | | |
| Uraninite | UO ₂ | √ | -- | √ | √ | √ |
| Coffinite | U(SiO ₄) _{1-x} (OH) _{4x} | √ | √ | -- | √ | -- |
| Andersonite | Na ₂ Ca(UO ₂)(CO ₃) ₃ · 6H ₂ O | -- | √ | √ | -- | -- |
| Torbernite | Cu(UO ₂) ₂ (PO ₄) ₂ · 12H ₂ O | -- | √ | -- | √ | √ |
| Tyuyamunite | Ca(UO ₂) ₂ V ₂ O ₈ · (5-8)H ₂ O | -- | -- | √ | √ | √ |
| Carnotite | K ₂ (UO ₂) ₂ (VO ₄) ₂ · 3H ₂ O | -- | √ | √ | -- | -- |
| Uranophane | (Ca(UO ₂) ₂ (SiO ₃ OH) ₂ · 5H ₂ O) | √ | √ | √ | √ | -- |
| Schoepfite | (UO ₂) ₈ O ₂ (OH) ₁₂ · 12(H ₂ O) | √ | -- | -- | -- | -- |
| Autunite | Ca(UO ₂) ₂ (PO ₄) ₂ · 10-12H ₂ O | √ | √ | √ | √ | √ |

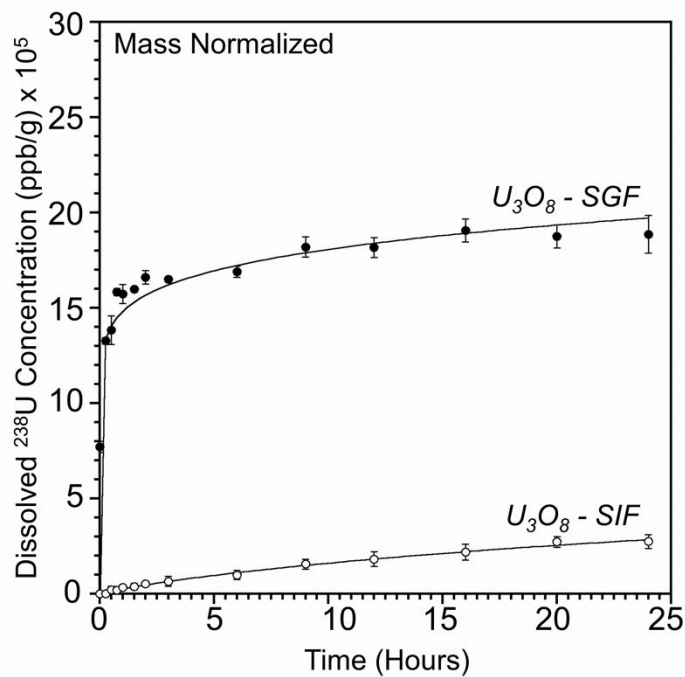


Figure 1: The mass normalized dissolution of uranium from U₃O₈ in SGF (closed marker) and SIF (open marker)

The leaching of uranium in the two simulated gastrointestinal fluids was first investigated with the NIST U₃O₈ standard. The obtained dissolution of U in simulated gastric fluid (SGF) is $(18.87 \pm 0.99) \times 10^5$ ppb/g, whereas that of SIF was $(2.75 \pm 0.36) \times 10^5$ ppb/g. The average rate of dissolution of U was calculated using the data collected within the first hour of reaction. They are $15.7 \times 10^5 \pm 0.5 \times 10^5 \mu\text{g L}^{-1}\text{g}^{-1} \text{h}^{-1}$ and $5.2 \times 10^4 \pm 0.8 \times 10^4 \mu\text{g L}^{-1}\text{g}^{-1}\text{h}^{-1}$, respectively, for SGF and SIF solutions (**Table 3**). The higher dissolution of uranium in the SGF solution than in the SIF solution was expected because the pH of the SGF solution (1.6) is lower than that of SIF solution (6.5). Minerals become more soluble in acidic environments than in basic environments because of the proton-promoted mechanism.^{42,43} However, pH plays a vital role in uranium complexation and in speciation and precipitation reactions, therefore, depending on the sample/ fluid composition, the solubility trends can be different.^{43–45}

Table 3: The average rates of U dissolution and the %U dissolved upon 24-hour exposure.

| Sample | Averaged rates of U dissolution for 1 st 1 hours ($\mu\text{g L}^{-1}\text{g}^{-1} \text{h}^{-1}$) | | %U dissolved upon 24-hour exposure | |
|-------------------------------|--|-----------------------------|---------------------------------------|-------|
| | SGF | SIF | SGF | SIF |
| U ₃ O ₈ | $(15.7 \pm 0.5) \times 10^5$ | $(5.2 \pm 0.8) \times 10^4$ | 22.19 | 3.24 |
| St Anthony Sediments | $(36.0 \pm 0.8) \times 10^2$ | 415.5 ± 35.4 | 6.38 | 1.52 |
| St Anthony Rocks | $(2.0 \pm 0.4) \times 10^5$ | $(1.4 \pm 0.2) \times 10^4$ | 90.63 | 20.84 |
| Site K | 27.4 ± 2.8 | 312.1 ± 60.2 | 0.16 | 2.79 |
| Site L | 15.8 ± 1.6 | 29.9 ± 3.3 | 0.51 | 0.58 |
| Site M | 57.0 ± 0.9 | 40.8 ± 2.4 | 1.15 | 2.19 |

In the next step, the uranium dissolution capacity from the five different natural dust and sediment samples was investigated. **Figure 2** represents the mass normalized dissolutions of U from different sample sites in both SGF and SIF fluids. The dissolution of uranium by each fluid varies for each sample site, and it varies between the two fluids for a given site. The rate of uranium dissolution in SGF follows as St. A. R > St. A. S > Site M > Site K > Site L, whereas for SIF, St. A. R > St. A. S > Site K > Site M > Site L. These differences in dissolution within the same fluid can arise for several reasons such as particle sizes, surface area, available %U in particles, and their mineralogy. In an attempt to eliminate the impacts from surface area and particle sizes, the observed extent of dissolutions was normalized to their specific surface area (**Supporting Information, Figure S4**). However, the observed trends remained the same. Therefore, the extent of dissolution was further normalized to the total uranium present in each sample (**Figure 3**). Following these normalizations, the extent of U dissolution in both fluids was still significantly

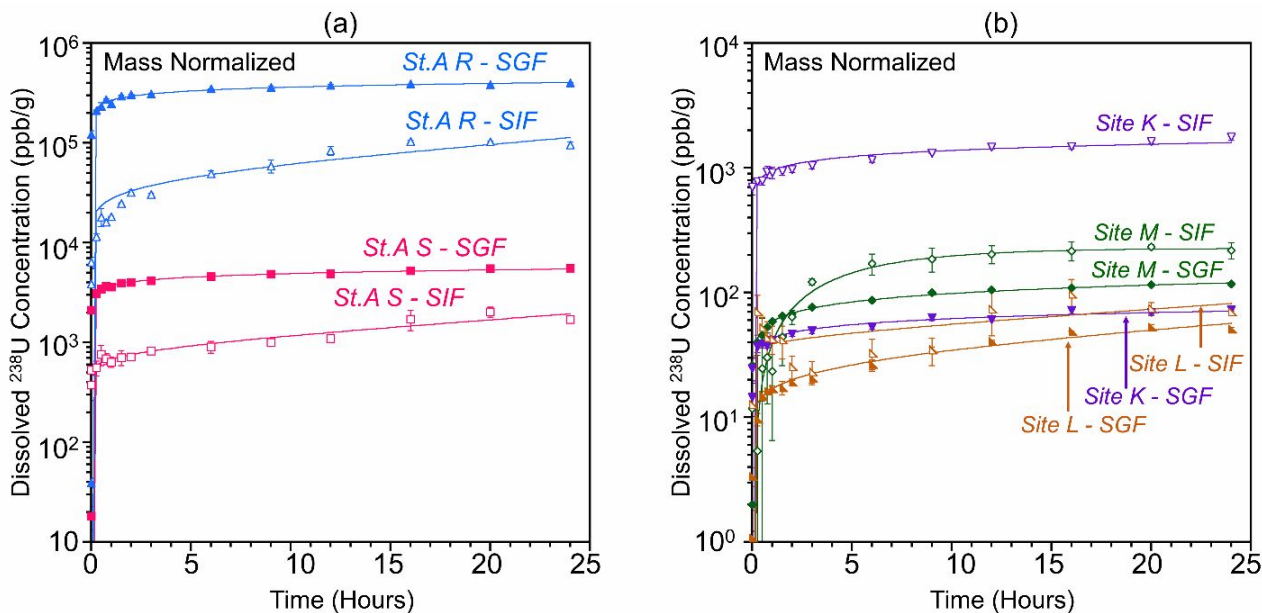


Figure 2: The mass normalized dissolutions of uranium from natural dust and sediment samples in SGF (closed markers) and SIF (open markers)

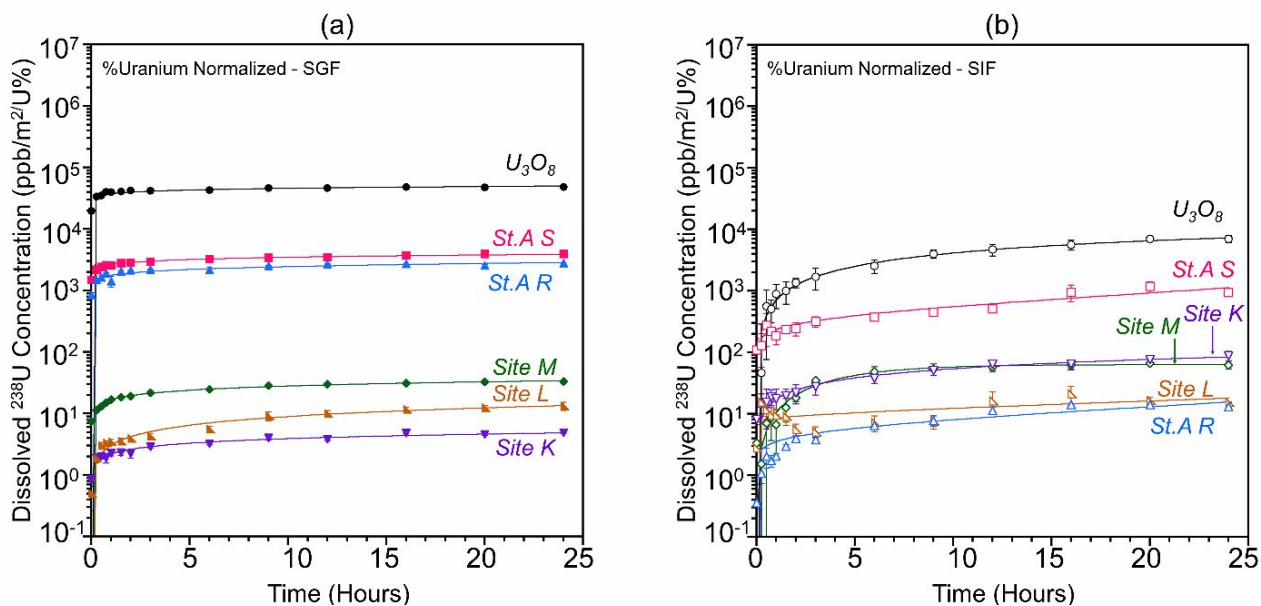


Figure 3: The %U normalized dissolutions of uranium from U_3O_8 and natural dust and sediment samples in (a) SGF (closed markers) and (b) SIF (open markers.)

different and can be attributed to factors such as compositional and mineralogical differences in these dust and sediment samples. The %U dissolved in SGF solution after exposure are 6.38%, 90.63%, 0.16%, 0.51%, and 1.15% for St. A. sediment, St. A. rock, Sites K, L, and M, respectively, whereas those in SIF solution are 1.52%, 20.84%, 2.79%, 0.58%, and 2.19%, respectively (**Table 3**). The rate of uranium dissolution as calculated from the first hour shows higher initial rates in

1
2
3 the SGF solution than SIF solution for St. A. R., St. A. S., and Site M, whereas Sites K and L have
4 higher initial rates of U dissolution in SIF solution than SGF solution (**Table 3**).
5
6

7 Furthermore, unlike for U_3O_8 , the samples from sites K, L, and M dissolved more uranium in the
8 SIF solution than SGF solution. However, the samples from the St. Anthony mine (sediment and
9 rock samples) dissolved more in SGF solution than in SIF solution, similar to U_3O_8 . The ratio of
10 dissolved U in SGF to SIF was calculated and added to the Supporting Information (**Table S3**).
11 The samples from the St. Anthony mine also showed similar dissolution trends to U_3O_8 in previous
12 studies with simulated lung fluids.³⁴ The post-pH analysis revealed that the changes in the pH after
13 the reaction were slight, and it was attributed to the differences in the amount of dolomite present.
14 (Please see Supporting Information). Many studies suggest that the dissolved uranium in the
15 gastrointestinal tract can cause immune suppressions and can be linked to the autoimmunity,
16 cardiovascular, and neurological disorders and cancers observed among the populations living in
17 the vicinity of uranium mines.^{3,5,6,46} Therefore, the dust-treated GIT solutions were analyzed for
18 dissolved uranium speciation. The dust- and sediment-treated SGIF did not develop a strong
19 orange coloration, which would indicate the presence of UO_2^{2+} . This differs from our previous
20 studies in simulated lung fluids where the uranyl cation was calorimetrically detected.³⁴ However,
21 from a separate series of experiments with larger quantities of dust and sediment, the uranyl cation
22 was identified as a dissolved uranium species. (**Supporting Information**) Therefore, uranium
23 constituents on inhaled dust particles may react with gastrointestinal fluids upon entering the
24 digestive tract and form uranyl cation and other complex dissolved uranium species.
25
26
27
28
29
30

31 **Computational Calculations of Uranium Solubility in Simulated Gastrointestinal Fluids and** 32 **Impact of Particle Mineralogy** 33

34 To better understand the impact of mineralogy on the U dissolution process in the SGIF, a series
35 of computational calculations were conducted to determine the dissolved U constituents. **Figure 4**
36 indicates the ratio of the calculated equilibrium U concentrations for each natural sample in SGF
37 and SIF solutions. Similar to bench experiments, the computational calculations suggest that both
38 St. A Rock and St. A Sediment samples are more soluble in the SGF solution than in the SIF
39 solution. In contrast, samples from Sites K, L, and M are more soluble in the SIF solution than in
40 the SGF solution. These concentrations are St. A. Rock (5.8130×10^{-1} M), St. A. Sediment (4.3100
41 $\times 10^{-3}$ M), Site L (9.2700×10^{-4} M), Site M (7.3000×10^{-4} M), and Site K (7.0000×10^{-4} M) for
42 the SGF solution. The concentrations for the SIF solution are St. A. Rock (5.5430×10^{-1} M), St.
43 A. Sediment (9.0000×10^{-4} M), Site M (7.4000×10^{-3} M), Site K (4.0000×10^{-3} M), and Site L
44 (7.5000×10^{-3} M). Further, the speciation analysis suggests that practically all dissolved uranium
45 is in the U(VI) oxidation state and represents a mixture of various aqueous uranyl complexes such
46 as uranyl carbonate (e.g., $[UO_2(CO_3)_3]^{4-}$ or $[UO_2(CO_3)_2]^{2-}$) or uranyl phosphate (e.g.,
47 $[UO_2(HPO_4)_2]^{2-}$) complexes. Deposited uranium or solid uranium has shown affinity toward
48 carbonate and bicarbonate in different environments.⁴⁷ The carbonates in this reaction can be
49 derived from either dolomite or andersonite in the samples. In contrast, phosphate can be derived
50 from uranium-phosphate minerals such as autunite or torbernite as well as from the lecithin in the
51
52
53
54
55
56
57

reaction medium. The concentration of phosphate can control the speciation of dissolved uranium.⁴³ Therefore, it is recommended to consider the phosphate mineralogy and speciation in future solid-uranium inhalation and digestion studies. Additionally, both SGF and SIF solutions, when reacted with St. A. R., contained $[(\text{UO}_2)_2(\text{OH})_2]^{2+}$ as another major dissolved uranium species. All solutions contained un-complexed UO_2^{2+} and $[\text{UO}_2\text{H}_3\text{SiO}_4]^+$ as minor components.

After modeling the experimentally observed SGF/SIF ratio of dissolved uranium concentrations, we calculated the uranium solubility for each mineral phase to understand their behavior in the simulated gastrointestinal fluids. All uranium minerals tested except andersonite favored higher dissolution in SGF over SIF solutions. The calculated concentrations in mol/dm^3 for SGF vs SIF solutions are autunite (2.00×10^{-2} , 5.53×10^{-4}), torbernite (2.00×10^{-2} , 2.29×10^{-4}), uranophane (1.91×10^{-2} , 5.93×10^{-6}), U_3O_8 (1.44×10^{-2} , 8.61×10^{-6}), schoepite (1.00×10^{-2} , 1.93×10^{-5}), andersonite (6.76×10^{-3} , 9.87×10^{-3}), tyuyamunite (6.18×10^{-3} , 7.49×10^{-6}), carnotite (4.70×10^{-3} , 8.51×10^{-6}), coffinite (1.99×10^{-9} , 1.88×10^{-11}), and uraninite (1.99×10^{-9} , 1.89×10^{-11}). As revealed from the calculations, coffinite and uraninite are extremely insoluble in the tested conditions. Further, the lower dissolutions observed in the SIF solution than in the SGF solution are clear evidence that experimentally observed dissolution trends are an outcome of combined sample mineralogy rather than the singular impact of one mineral. The speciation analysis suggested that un-complexed UO_2^{2+} is the primary dissolved uranium species when carbonate and phosphate sources are missing.

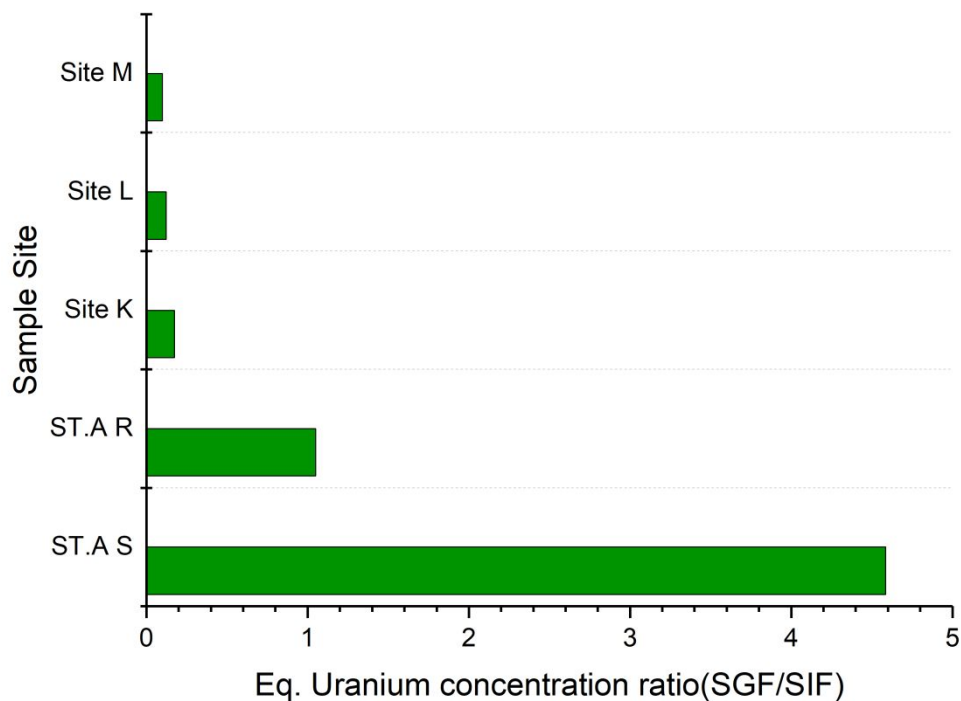


Figure 4: SGF/ SIF ratio of calculated equilibrium U concentrations.

As kaolinite was identified in all the analyzed dust and sediment samples, each single-phase uranium mineral was combined with 1.000 mol of kaolinite, and dissolved uranium concentrations were recalculated. Kaolinite ($\text{Al}_2\text{Si}_2\text{O}_5(\text{OH})_4$) is a naturally occurring common clay mineral, a 1:1 layered aluminosilicate structure consisting of alternating silica and alumina sheets.^{48,49} In aqueous solutions, kaolinite surface hydroxylates and participates in surface reactions.⁵⁰ Upon adding kaolinite, the SGF/SIF ratio was decreased for all the minerals (**Figure 5 & Table S6**) except andersonite. Further, these data implied the presence of kaolinite could significantly change the extent of uranium dissolution from these minerals inside the human gastrointestinal tract. Then, a similar recalculation was conducted for each uranium mineral mixing with 1.000 mol of microcline. Microcline is a potassium-rich alkali feldspar mineral (KAlSi_3O_8) identified in all the samples except the St. Anthony sediment sample. The addition of microcline decreased the SGF/SIF ratio for all tested minerals. Further, the SGF/SIF ratio dropped below 1 for torbernite, coffinite, and uraninite mixtures with microcline, showing the presence of microcline greatly favors higher solubility in SIF solution. Overall, non-U-minerals such as kaolinite and microcline can impact the dissolution of uranium minerals in simulated gastrointestinal fluids.

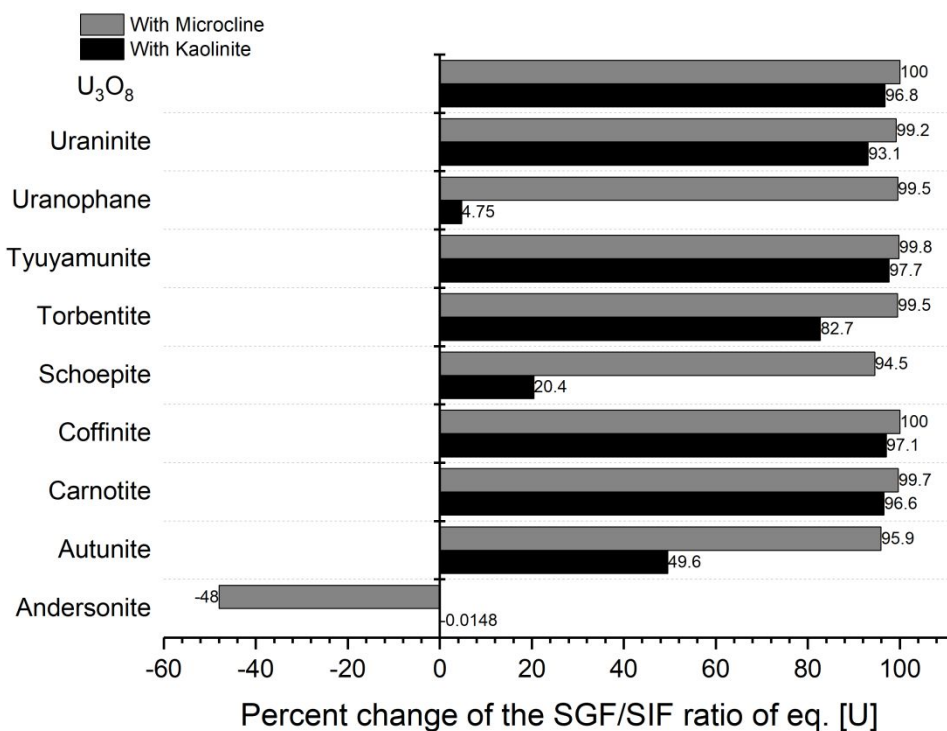


Figure 5: Percent changes of single-phase uranium solubility ratios of SGF/SIF as a function of either kaolinite or microcline. The positive numbers indicate a decrease in concentration while the negative numbers indicate an increase in concentration.

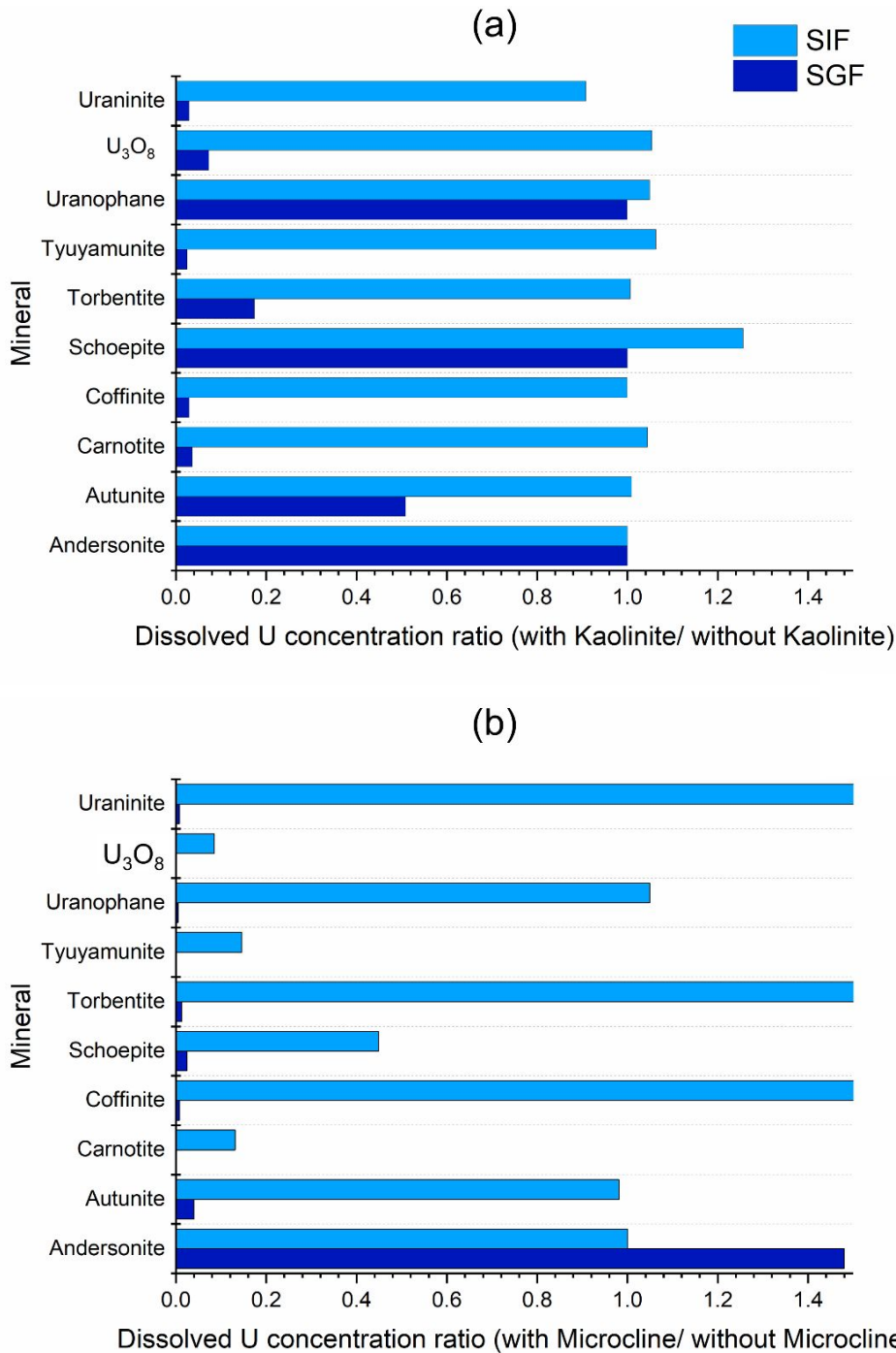


Figure 6: Dissolved U concentration ratios for each mineral in each SGIF. (a) The ratio of U dissolution when kaolinite is present to the U dissolution when kaolinite is not present (b) The ratio of U dissolution when microcline is present to the U dissolution when microcline is not present.

Figure 6 and Supporting Information Figure S7 represents the dissolved uranium ratio in each fluid with and without kaolinite or microcline. The solubility of uranium in the SGF solution from

1
2
3 all the tested minerals, except for andersonite and uranophane, decreases upon adding kaolinite. In
4 contrast, with the addition of microcline, the uranium solubility decreases for all minerals except
5 andersonite. The solubility of andersonite and uranophane in the SGF solution was not affected by
6 the addition of kaolinite. The decrease in solubility could be due to the ability of hydroxyl groups
7 in surfaces to react with protons in the acidic SGF solution and the ability of metal centers to
8 interact with anions, thereby effectively decreasing the proton-promoted uranium dissolution.
9 However, the solubility of andersonite, a uranium carbonate mineral, in the SGF solution was
10 increased with the addition of microcline.
11
12
13

14 Unlike in the highly acidic SGF solution (pH = 1.6), the uranium solubility in the SIF solution (pH
15 = 6.5) showed mixed trends with the addition of either kaolinite or microcline. While andersonite
16 solubility was not affected by the presence of kaolinite, the uranium solubility of both uraninite
17 and coffinite decreased in the SIF solution. All the other tested minerals showed enhancements in
18 the uranium solubility. The dissolved uranium concentrations in SIF solutions were increased for
19 coffinite, torbernite, uranophane, and uraninite in the presence of microcline, whereas all other
20 minerals except andersonite showed a decrease in dissolved uranium concentration. The calculated
21 trends imply that the pH and composition of the solution, along with the mineralogy of particles,
22 affect uranium. It is important to note that in the current study, the impact of kaolinite or microcline
23 on uranium dissolution is evident when the kaolinite to uranium mineral ratio (microcline to
24 uranium mineral ratio) is 1.000:0.001. This ratio was used to simulate the presence of excess
25 kaolinite or microcline in the system. Therefore, it is possible that uranium solubility can further
26 change by varying the ratio of these minerals. Additionally, the higher uranium solubility in SIF
27 solution for the samples from sites K, L, and M than in SGF solution may be attributed to certain
28 mineralogical and compositional features observed, such as the presence of tyuyamunite and a
29 higher percentage of autunite. Further, the variable quantities of torbernite and carnotite in these
30 samples can play a role in enhanced U leaching in SIF solution.
31
32
33
34
35
36
37

38 **Conclusion**

39 In the current study, the solubility of uranium from relatively larger-sized inhaled particles in
40 human gastrointestinal tract conditions was investigated using simulated gastric and intestinal
41 fluids in the fasted state. The uranium from these dust and sediment samples collected near Jackpile
42 and St. Anthony mines in NM might solubilize in human gut conditions, potentially leading to
43 subsequent absorption. The samples from the sites St. A. (sediment and rock) are more soluble in
44 human stomach-like conditions (as simulated by SGF), whereas samples from sites K, L, and M
45 are more soluble in human intestine-like conditions (as simulated by SIF). Further, through
46 experimentally obtained mineralogical information and computational geochemical calculations,
47 we reported that these solubility differences are partly due to the mineralogical differences. The
48 combined mineralogy, and the presence of non-uranium minerals (kaolinite and microcline)
49 influence in the extent of uranium dissolution from these minerals. The most prevalent oxidation
50 state of dissolved uranium was computationally determined as +6. Therefore, we report that the
51 solubility of solid uranium in the human digestive tract after inhalation is possible and that the
52
53
54
55
56
57

1
2
3 extent of uranium concentration and its speciation depends on the site-specific mineralogy. Thus,
4 these factors should be weighed into the toxicological assessments. Further, considering the
5 scarcity of studies on the impact of dissolved uranium on gut microbiota, the authors suggest
6 furthering research to understand how human gut microbiota will interact with the uranium
7 contained in inhaled dust.
8
9

10 **Conflict of Interest**

11
12 There are no conflicts to declare.
13

14 **Acknowledgment**

15
16 Research reported in this publication was partially supported by an Institutional Development
17 Award (IDeA) from the National Institute of General Medical Sciences of the National Institutes
18 of Health under grant number P20GM103451 and NM EPSCoR under the National Science
19 Foundation/EPSCoR Award No. IIA-1301346. The authors would also like to thank
20 <https://smart.servier.com/> for granting permission to use their human body images in the graphical
21 abstract at no cost.
22
23
24

25 **Author Information**

26
27 **Corresponding Author** *G. Rubasinghege. E-mail: gayan.rubasinghege@nmt.edu
28

29 **ORCID**

30
31 Eshani Hettiarachchi: 0000-0003-4293-770X
32

33 Milton Das: 0000-0002-8944-6484
34

35 Daniel Cadol: 0000-0002-4408-8548
36

37 Bonnie A. Frey: 0000-0002-0718-4645
38

39 Gayan Rubasinghege: 0000-0002-2089-6807
40

41 **Associated Content**

42
43 Supplementary Information contains the compositions of the simulated gastrointestinal fluids, a
44 map of the study area, SEM images, particle-size distribution of the samples, computation
45 calculations, mineralogy input for the computational calculations, and uranyl cation detection.
46
47

48 **References:**

- 49
50 (1) Briner, W. The Toxicity of Depleted Uranium. *Int. J. Environ. Res. Public Health* **2010**, *7*,
51 303–313. <https://doi.org/10.3390/ijerph7010303>.
52
53 (2) Jiang, G. C. T.; Aschner, M. Depleted Uranium. In *Handbook of Toxicology of Chemical*
54 *Warfare Agents: Second Edition*; Elsevier Inc., 2015; pp 447–460.
55 <https://doi.org/10.1016/B978-0-12-800159-2.00033-6>.
56
57
58
59
60

- 1
2
3 (3) Medina, S.; Lauer, F. T.; Castillo, E. F.; Bolt, A. M.; Ali, A.-M. S.; Liu, K. J.; Burchiel, S.
4 W. Exposures to Uranium and Arsenic Alter Intraepithelial and Innate Immune Cells in the
5 Small Intestine of Male and Female Mice. *Toxicol. Appl. Pharmacol.* **2020**, *403*, 115155.
6 <https://doi.org/10.1016/j.taap.2020.115155>.
- 7
8 (4) Hughes, M. E.; Waite, L. J. Health in Household Context: Living Arrangements and Health
9 in Late Middle Age. *J. Health Soc. Behav.* **2002**, *43* (1), 1. <https://doi.org/10.2307/3090242>.
- 10
11 (5) Erdei, E.; Shuey, C.; Pacheco, B.; Cajero, M.; Lewis, J.; Rubin, R. L. Elevated
12 Autoimmunity in Residents Living near Abandoned Uranium Mine Sites on the Navajo
13 Nation. *J. Autoimmun.* **2019**, *99*, 15–23. <https://doi.org/10.1016/j.jaut.2019.01.006>.
- 14
15 (6) Ferrario, D.; Gribaldo, L.; Hartung, T. Arsenic Exposure and Immunotoxicity: A Review
16 Including the Possible Influence of Age and Sex. *Curr. Environ. Heal. Reports* **2016**, *3* (1),
17 1–12. <https://doi.org/10.1007/s40572-016-0082-3>.
- 18
19 (7) Stearns, D. M.; Yazzie, M.; Bradley, A. S.; Coryell, V. H.; Shelley, J. T.; Ashby, A.;
20 Asplund, C. S.; Lantz, R. C. Uranyl Acetate Induces Hprt Mutations and Uranium-DNA
21 Adducts in Chinese Hamster Ovary EM9 Cells. *Mutagenesis* **2005**, *20*, 417–423.
22 <https://doi.org/10.1093/mutage/gei056>.
- 23
24 (8) Pereira, S.; Camilleri, V.; Floriani, M.; Cavalié, I.; Garnier-Laplace, J.; Adam-Guillermin,
25 C. Genotoxicity of Uranium Contamination in Embryonic Zebrafish Cells. *Aquat. Toxicol.*
26 **2012**, *109*, 11–16. <https://doi.org/10.1016/j.aquatox.2011.11.011>.
- 27
28 (9) Hsieh, P.; Yamane, K. DNA Mismatch Repair: Molecular Mechanism, Cancer, and Ageing.
29 *Mech. Ageing Dev.* **2008**, *129* (7–8), 391–407. <https://doi.org/10.1016/j.mad.2008.02.012>.
- 30
31 (10) Schneider, J.; Philipp, M.; Pamini, P.; Dörk, T.; Voitowitz, H. ATM Gene Mutations in
32 Former Uranium Miners of SDAG Wismut: A Pilot Study. *Oncol. Rep.* **2007**, *17*, 477–482.
- 33
34 (11) Periyakaruppan, A.; Kumar, F.; Sarkar, S.; Sharma, C. S.; Ramesh, G. T. Uranium Induces
35 Oxidative Stress in Lung Epithelial Cells. *Arch. Toxicol.* **2007**, *81* (6), 389–395.
36 <https://doi.org/10.1007/s00204-006-0167-0>.
- 37
38 (12) Orona, N. S.; Tasat, D. R. Uranyl Nitrate-Exposed Rat Alveolar Macrophages Cell Death:
39 Influence of Superoxide Anion and TNF α Mediators. *Toxicol. Appl. Pharmacol.* **2012**, *261*
40 (3), 309–316. <https://doi.org/10.1016/j.taap.2012.04.022>.
- 41
42 (13) Thiebault, C.; Carriere, M.; Milgram, S.; Simon, A.; Avoscan, L.; Gouget, B. Uranium
43 Induces Apoptosis and Is Genotoxic to Normal Rat Kidney (NRK-52E) Proximal Cells.
44 *Toxicol. Sci.* **2007**, *98* (2), 479–487. <https://doi.org/10.1093/toxsci/kfm130>.
- 45
46 (14) Monleau, M.; De Méo, M.; Frelon, S.; Paquet, F.; Donnadiou-Claraz, M.; Duménil, G.;
47 Chazel, V. Distribution and Genotoxic Effects After Successive Exposure to Different
48 Uranium Oxide Particles Inhaled by Rats. *Inhal. Toxicol.* **2006**, *18* (11), 885–894.
49 <https://doi.org/10.1080/08958370600822524>.
- 50
51 (15) Wilson, A.; Velasco, C. A.; Herbert, G. W.; Lucas, S. N.; Sanchez, B. N.; Cerrato, J. M.;
52 Spilde, M.; Li, Q.-Z.; Campen, M. J.; Zychowski, K. E. Mine-Site Derived Particulate
53 Matter Exposure Exacerbates Neurological and Pulmonary Inflammatory Outcomes in an
54 Autoimmune Mouse Model. *J. Toxicol. Environ. Heal. Part A* **2021**, 1–15.
- 55
56
57
58
59
60

- 1
2
3 <https://doi.org/10.1080/15287394.2021.1891488>.
- 4
- 5 (16) Asic, A.; Kurtovic-Kozaric, A.; Besic, L.; Mehinovic, L.; Hasic, A.; Kozaric, M.; Hukic,
6 M.; Marjanovic, D. Chemical Toxicity and Radioactivity of Depleted Uranium: The
7 Evidence from in Vivo and in Vitro Studies. *Environ. Res.* **2017**, *156*, 665–673.
8 <https://doi.org/10.1016/j.envres.2017.04.032>.
- 9
- 10 (17) Kastury, F.; Smith, E.; Juhasz, A. L. A Critical Review of Approaches and Limitations of
11 Inhalation Bioavailability and Bioaccessibility of Metal(Loid)s from Ambient Particulate
12 Matter or Dust. *Sci. Total Environ.* **2017**, *574*, 1054–1074.
13 <https://doi.org/10.1016/j.scitotenv.2016.09.056>.
- 14
- 15 (18) Stine, K. .; Brown, T. *Principles of Toxicology*, 1st ed.; CRC Lewis: New York, 2010.
- 16
- 17 (19) Alpofoad, J. A. H.; Davidson, C. M.; Littlejohn, D. A Novel Two-Step Sequential
18 Bioaccessibility Test for Potentially Toxic Elements in Inhaled Particulate Matter
19 Transported into the Gastrointestinal Tract by Mucociliary Clearance. *Anal. Bioanal. Chem.*
20 **2017**, *409* (12), 3165–3174. <https://doi.org/10.1007/s00216-017-0257-2>.
- 21
- 22 (20) Martin, R.; Dowling, K.; Pearce, D.; Sillitoe, J.; Florentine, S. Health Effects Associated
23 with Inhalation of Airborne Arsenic Arising from Mining Operations. *Geosciences* **2014**, *4*
24 (3), 128–175. <https://doi.org/10.3390/geosciences4030128>.
- 25
- 26 (21) Fahy, J. V.; Dickey, B. F. Airway Mucus Function and Dysfunction. *N. Engl. J. Med.* **2010**,
27 *363* (23), 2233–2247. <https://doi.org/10.1056/NEJMra0910061>.
- 28
- 29 (22) Smith, J. R. .; Etherington, G.; Shutt, A. L.; Youngman, M. J. A Study of Aerosol
30 Deposition and Clearance from the Human Nasal Passage. *Ann. Occup. Hyg.* **2002**, *46*, 309–
31 313. https://doi.org/10.1093/annhyg/46.suppl_1.309.
- 32
- 33 (23) Guney, M.; Bourges, C. M. J.; Chapuis, R. P.; Zagury, G. J. Lung Bioaccessibility of As,
34 Cu, Fe, Mn, Ni, Pb, and Zn in Fine Fraction (< 20 Mm) from Contaminated Soils and Mine
35 Tailings. *Sci. Total Environ.* **2017**, *579*, 378–386.
36 <https://doi.org/10.1016/j.scitotenv.2016.11.086>.
- 37
- 38 (24) Brugge, D. Uranium. In *Encyclopedia of Toxicology: Third Edition*; Elsevier, 2014; pp 883–
39 884. <https://doi.org/10.1016/B978-0-12-386454-3.00071-3>.
- 40
- 41 (25) Frelon, S.; Houpert, P.; Lepetit, D.; Paquet, F. The Chemical Speciation of Uranium in
42 Water Does Not Influence Its Absorption from the Gastrointestinal Tract of Rats. *Chem.*
43 *Res. Toxicol.* **2005**, *18* (7), 1150–1154. <https://doi.org/10.1021/tx049662i>.
- 44
- 45 (26) Marques, M. R. C.; Loebenberg, R.; Almukainzi, M. Simulated Biological Fluids with
46 Possible Application in Dissolution Testing. *Dissolution Technol.* **2011**, *18* (3), 15–28.
47 <https://doi.org/10.14227/DT180311P15>.
- 48
- 49 (27) McGuigan, M. A. Chronic Poisoning: Trace Metals and Others. In *Goldman's Cecil*
50 *Medicine: Twenty Fourth Edition*; Elsevier Inc., 2011; Vol. 1, pp 88–95.
51 <https://doi.org/10.1016/B978-1-4377-1604-7.00021-X>.
- 52
- 53 (28) Breton, J.; Massart, S.; Vandamme, P.; De Brandt, E.; Pot, B.; Foligné, B. Ecotoxicology
54 inside the Gut: Impact of Heavy Metals on the Mouse Microbiome. *BMC Pharmacol.*
55
- 56
- 57
- 58
- 59
- 60

- Toxicol.* **2013**, *14* (1), 62. <https://doi.org/10.1186/2050-6511-14-62>.
- (29) Chi, L.; Bian, X.; Gao, B.; Ru, H.; Tu, P.; Lu, K. Sex-Specific Effects of Arsenic Exposure on the Trajectory and Function of the Gut Microbiome. *Chem. Res. Toxicol.* **2016**, *29* (6), 949–951. <https://doi.org/10.1021/acs.chemrestox.6b00066>.
- (30) Chi, L.; Bian, X.; Gao, B.; Tu, P.; Ru, H.; Lu, K. The Effects of an Environmentally Relevant Level of Arsenic on the Gut Microbiome and Its Functional Metagenome. *Toxicol. Sci.* **2017**, *160* (2), 193–204. <https://doi.org/10.1093/toxsci/kfx174>.
- (31) Tsiaoussis, J.; Antoniou, M. N.; Koliarakis, I.; Mesnage, R.; Vardavas, C. I.; Izotov, B. N.; Psaroulaki, A.; Tsatsakis, A. Effects of Single and Combined Toxic Exposures on the Gut Microbiome: Current Knowledge and Future Directions. *Toxicol. Lett.* **2019**, *312*, 72–97. <https://doi.org/10.1016/j.toxlet.2019.04.014>.
- (32) Cleveland, D.; Hinck, J. E.; Lankton, J. S. Elemental and Radionuclide Exposures and Uptakes by Small Rodents, Invertebrates, and Vegetation at Active and Post-Production Uranium Mines in the Grand Canyon Watershed. *Chemosphere* **2021**, *263*, 127908. <https://doi.org/10.1016/j.chemosphere.2020.127908>.
- (33) Zychowski, K. E.; Kodali, V.; Harmon, M.; Sanchez, B.; Suarez, Y. O.; Cerrato, J. M.; Muttill, P.; Brearley, A.; Ali, A.-M. M.; Lin, Y.; et al. Respirable Uranyl-Vanadate Containing Particulate Matter Derived from a Legacy Uranium Mine Site Exhibits Potentiated Cardiopulmonary Toxicity. *Toxicol. Sci.* **2018**, *164* (1), 101–114. <https://doi.org/10.1093/toxsci/kfy064/4962180>.
- (34) Hettiarachchi, E.; Paul, S.; Cadol, D.; Frey, B.; Rubasinghege, G. Mineralogy Controlled Dissolution of Uranium from Airborne Dust in Simulated Lung Fluids (SLFs) and Possible Health Implications. *Environ. Sci. Technol. Lett.* **2019**, *6* (2), 62–67. <https://doi.org/10.1021/acs.estlett.8b00557>.
- (35) Parkhurst, D.; Appelo, C. Description of Input and Examples for PHREEQC Version 3-A Computer Program for Speciation, Batch-Reaction, One-Dimensional Transport, and Inverse Geochemical Calculations. USGS 2013.
- (36) Brown, R. D. Geochemistry and Transport of Uranium-Bearing Dust at Jackpile Mine, Laguna, New Mexico, New Mexico Institute of Mining and Technology, 2017.
- (37) Zhu, J. H.; Zhao, X.; Yang, J.; Tan, Y. T.; Zhang, L.; Liu, S. P.; Liu, Z. F.; Hu, X. L. Selective Colorimetric and Fluorescent Quenching Determination of Uranyl Ion via Its Complexation with Curcumin. *Spectrochim. Acta - Part A Mol. Biomol. Spectrosc.* **2016**, *159*, 146–150. <https://doi.org/10.1016/j.saa.2016.01.021>.
- (38) Wilton, T. Uranium Deposits at the Cebolleta Project, Laguna Mining District, Cibola County, New Mexico. *New Mex. Geol.* **2017**, *39* (1), 1–10.
- (39) Kogianni, E.; Kouras, A.; Samara, C. Indoor Concentrations of PM_{2.5} and Associated Water-Soluble and Labile Heavy Metal Fractions in Workplaces: Implications for Inhalation Health Risk Assessment. *Environ. Sci. Pollut. Res.* **2020**. <https://doi.org/10.1007/s11356-019-07584-8>.
- (40) Chen, L. C.; Lippmann, M. Effects of Metals within Ambient Air Particulate Matter (PM)

- on Human Health. *Inhal. Toxicol.* **2009**, *21* (1), 1–31. <https://doi.org/10.1080/08958370802105405>.
- (41) Mercer, R. R.; Scabilloni, J. F.; Wang, L.; Battelli, L. A.; Antonini, J. M.; Roberts, J. R.; Qian, Y.; Sisler, J. D.; Castranova, V.; Porter, D. W.; et al. The Fate of Inhaled Nanoparticles: Detection and Measurement by Enhanced Dark-Field Microscopy. *Toxicol. Pathol.* **2018**. <https://doi.org/10.1177/0192623317732321>.
- (42) Wang, Z.; Fu, H.; Zhang, L.; Song, W.; Chen, J. Ligand-Promoted Photoreductive Dissolution of Goethite by Atmospheric Low-Molecular Dicarboxylates. *J. Phys. Chem. A* **2017**. <https://doi.org/10.1021/acs.jpca.6b09160>.
- (43) Perdrial, N.; Vázquez-Ortega, A.; Wang, G.; Kanematsu, M.; Mueller, K. T.; Um, W.; Steefel, C. I.; O’Day, P. A.; Chorover, J. Uranium Speciation in Acid Waste-Weathered Sediments: The Role of Aging and Phosphate Amendments. *Appl. Geochemistry* **2018**, *89*, 109–120. <https://doi.org/10.1016/j.apgeochem.2017.12.001>.
- (44) Gonzalez-Estrella, J.; Meza, I.; Burns, A. J.; Ali, A.-M. S.; Lezama-Pacheco, J. S.; Lichtner, P.; Shaikh, N.; Fendorf, S.; Cerrato, J. M. Effect of Bicarbonate, Calcium, and PH on the Reactivity of As(V) and U(VI) Mixtures. *Environ. Sci. Technol.* **2020**, *54* (7), 3979–3987. <https://doi.org/10.1021/acs.est.9b06063>.
- (45) Guibal, E.; Roulph, C.; Le Cloirec, P. Uranium Biosorption by a Filamentous Fungus *Mucor Miehei* PH Effect on Mechanisms and Performances of Uptake. *Water Res.* **1992**, *26* (8), 1139–1145. [https://doi.org/10.1016/0043-1354\(92\)90151-S](https://doi.org/10.1016/0043-1354(92)90151-S).
- (46) Harmon, M. E.; Lewis, J.; Miller, C.; Hoover, J.; Ali, A.-M. S.; Shuey, C.; Cajero, M.; Lucas, S.; Zychowski, K.; Pacheco, B.; et al. Residential Proximity to Abandoned Uranium Mines and Serum Inflammatory Potential in Chronically Exposed Navajo Communities. *J. Expo. Sci. Environ. Epidemiol.* **2017**, *27* (4), 365–371. <https://doi.org/10.1038/jes.2016.79>.
- (47) Avasarala, S.; Torres, C.; Ali, A.-M. S.; Thomson, B. M.; Spilde, M. N.; Peterson, E. J.; Artyushkova, K.; Dobrica, E.; Lezama-Pacheco, J. S.; Cerrato, J. M. Effect of Bicarbonate and Oxidizing Conditions on U(IV) and U(VI) Reactivity in Mineralized Deposits of New Mexico. *Chem. Geol.* **2019**, *524* (June), 345–355. <https://doi.org/10.1016/j.chemgeo.2019.07.007>.
- (48) Alstadt, V. J.; Kubicki, J. D.; Freedman, M. A. Competitive Adsorption of Acetic Acid and Water on Kaolinite. *J. Phys. Chem. A* **2016**, *120* (42), 8339–8346. <https://doi.org/10.1021/acs.jpca.6b06968>.
- (49) Taha, M. H.; El-Maadawy, M. M.; Hussein, A. E. M.; Youssef, W. M. Uranium Sorption from Commercial Phosphoric Acid Using Kaolinite and Metakaolinite. *J. Radioanal. Nucl. Chem.* **2018**, *317* (2), 685–699. <https://doi.org/10.1007/s10967-018-5951-9>.
- (50) Doi, A.; Khosravi, M.; Ejtemaei, M.; Nguyen, T. A. H.; Nguyen, A. V. Specificity and Affinity of Multivalent Ions Adsorption to Kaolinite Surface. *Appl. Clay Sci.* **2020**, *190*, 105557. <https://doi.org/10.1016/j.clay.2020.105557>.